Available online at www.sciencedirect.com
ScienceDirect
Ceramics International 35 (2009) 3291–3299
CERAMICS INTERNATIONAL
www.elsevier.com/locate/ceramint

Electrically induced liquid infiltration for the synthesis of carbon/carbon–silicon carbide composite

Alexander S. Mukasyan *, Jeremiah D.E. White

Department of Chemical and Biomolecular Engineering, University of Notre Dame, 182 Fitzpatrick Hall, Notre Dame, IN 46556, USA

Received 18 March 2009; received in revised form 27 April 2009; accepted 23 May 2009
Available online 21 June 2009

Abstract

The electrically induced liquid infiltration (EILI) method for the synthesis of carbon/carbon–silicon carbide (C/C–SiC) materials was developed. The method involves Joule preheating of a porous carbon/carbon preform surrounded by silicon media, followed by silicon infiltration into the pore structure, and its reaction with carbon to form pore-free C/C–SiC composite. This technique is characterized by high heating rates (10^2–10^3 K/s) and short processing times (5–20 s), which distinguish it from conventional approaches. The influence of maximum treatment temperature, as well as preheating rate on the depth of infiltration, reaction kinetics, and the material microstructure was investigated. C/C–SiC composite with a compressive strength which was twice that of the initial C/C material was synthesized.

Keywords: B. Composites; D. SiC; E. Refractories; E. Wear parts; Liquid infiltration

1. Introduction

Silicon carbide–carbon (SiC–C) composites belong to an advanced class of materials widely used for aerospace [1–4] and performance braking applications [3,4]. They exhibit higher mechanical properties at elevated temperatures, as well as enhanced resistances to wear and oxidation over alternatives. First attempts to prepare carbon/carbon–silicon carbide (C/C–SiC) composite by infiltrating a carbon/carbon skeleton with liquid silicon were made in the mid-1970s [5,6]. The method that was developed requires the usage of specially coated, highly graphitized carbon fibers, which is not a cost efficient approach. Development of silicon carbide based advanced ceramics and composites continued in the 1980s [7,8] and 1990s [9–11]. More recently, the liquid silicon infiltration (LSI) process was developed which allows for the usage of uncoated and non-graphitized fibers [3]. This process involves the pyrolysis of carbon fiber reinforced plastic composites under an inert atmosphere at temperatures between 900 and 1650 °C in order to convert the polymer matrix to amorphous carbon, followed by infiltration of molten silicon at about 1600 °C, which fills the cracks and pores within a few minutes.

All of the above mentioned approaches require treating the materials for a relatively long time at high temperatures in order to form the composite of desired composition and microstructure. Also, the main question is whether or not the progressive ingress of molten silicon continues until the pores get filled and without damaging the fibers and inter-phase. In this paper, a so-called electrically induced liquid infiltration (EILI) method was developed and this critical question was addressed. It was demonstrated that EILI is a rapid (on the order of seconds), efficient method that leads to the formation of *pore-free C/C–SiC* composite with attractive mechanical properties.

2. Experimental

A detailed description of the apparatus used in this work can be found elsewhere [12]. Briefly, referring to Fig. 1a, the specimen to be processed is inserted into the reaction chamber (1), to be described later, and is held in place between two electrodes (2), which are connected to a direct current (DC) power supply (3). The electrodes are also part of the pneumatic system (4), which applies a uniaxial load to the sample. All operational parameters such as initial pressure (P_i) and final pressure (P_f), applied current

* Corresponding author. Tel.: +1 574 631 9825; fax: +1 574 631 8366.
E-mail address: amoukasi@nd.edu (A.S. Mukasyan).

0272-8842/$36.00
doi:10.1016/j.ceramint.2009.05.017

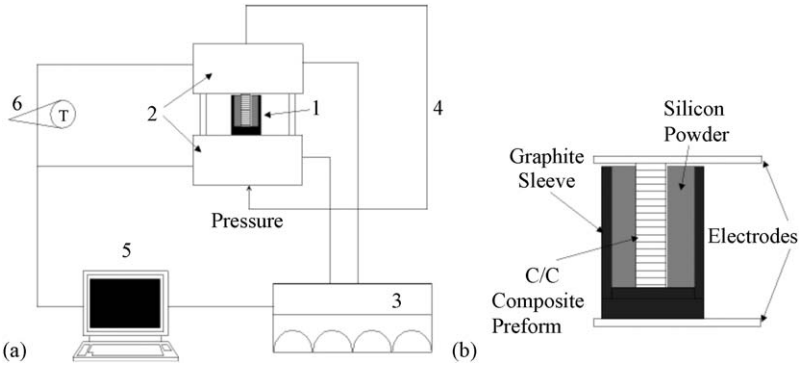

Fig. 1. (a) Schematic of apparatus used for EILI and (b) details of the reactive vessel.

(I_{max}), delay time before final pressure application (Δt_h), and others are defined with a programmable logic controller (5). Temperature can be measured with a thermocouple and high-speed infrared thermal imaging system (SC6000; FLIR Systems, North Billerica, MA) (6).

In this study, we began with a prefabricated carbon/carbon (C/C) composite, which was produced by Honeywell Aerospace (South Bend, IN). Layers of a felt-like carbon fiber ($\sim$10 μm in diameter) material are stitched together into an annular shape, forming a preform with high initial porosity (about 75%). The preform is placed in a furnace where it is treated at high temperatures in the presence of natural gas, during which additional carbon enters the pore structure by chemical vapor infiltration (CVI). Thus, after processing the C/C composite structure is composed of carbon fibers within a CVI carbon matrix. The density of the bulk material is $\rho = 2.0$ g/cm^3, while the fibers are $\rho = 1.75$ g/cm^3, and the matrix is $\rho = 2.1$ g/cm^3. Total *open porosity* is 15%. The cylindrical specimens used for this investigation were all cut from one large disc and had measurements of diameter $D_{C/C} = 10$ mm and length $l_{C/C} = 25$ mm. The silicon that was used was a 99% purity −325 mesh powder (Strem Chemicals, Newburyport, MA).

To prepare a composite, a C/C specimen was positioned in a graphite sleeve with inner diameter $D_{GI} = 18$ mm and outer diameter $D_{GO} = 25$ mm, as shown in Fig. 1b. The bottom end of the sleeve was capped with another piece of graphite, and the silicon powder was poured in, occupying the open space between the sleeve and C/C piece.

As DC passes through the C/C cylinder, it is preheated due to the electrical resistance of the material. The temperature rapidly (seconds) rises above the melting point (1687 K) of the surrounding silicon powder; it melts and, due to capillary forces, infiltrates the porous skeleton of the C/C composite. Finally, the infiltrated silicon reacts with carbon, forming silicon carbide.

In addition, the EILI approach was modified to form a protective SiC coating on the surface of C/C composite. In this case, instead of surrounding the C/C specimen with silicon powder in a graphite sleeve, a thin layer of slurry containing silicon powder was painted onto the surface and allowed to dry before heat-treating the sample.

Microstructures of the synthesized composite materials were examined with scanning electron microscopy (SEM) (EVO 50 Series; Zeiss, Peabody, MA), energy dispersive X-ray spectroscopy (EDS) (INCAx-sight Model 7636; Oxford Instruments, Concord, MA), and X-ray diffractometry (XRD) (Scintag X1 Advanced Diffraction System, Scintag Inc., Cupertino, CA). Mechanical properties were characterized by measuring the compressive strength of the synthesized materials on Universal Testing Machine (Series 900; Applied Test Systems, Butler, PA). The influences of different processing parameters, such as heating rate and maximum reaction temperature, on the infiltration rate, kinetics of chemical interaction, and microstructure formation are discussed in detail in the following section.

3. Results and discussion

3.1. Electrical preheating

In this study, electrical current (I) ranging from 300 to 600 A was used to preheat C/C specimens, while the maximum capability of the apparatus is 900 A. Typical temperature–time histories of the preheated samples for different applied currents are shown in Fig. 2a. It can be seen that this results in high heating rates, more specifically varying from 190 to 500 K/s. Also, the maximum, or saturation, temperature (T_m) that can be achieved was found to depend linearly on the value of the applied current (Fig. 2b). Finally, one should note that the sample temperature exceeds the melting point of silicon (1687 K) after 3–7 s of preheating, depending on the heating rate.

It is important to outline a couple of features of the EILI process, which distinguish it from conventional infiltration approaches. First, the C/C skeleton is preheated to temperatures much higher than the melting temperature of silicon. This is not the case when one, for example, immerses a porous composite into a crucible of liquid silicon and the skeleton remains at a lower temperature for a relatively long period of time. Second, the preheating time is very short (i.e. on the order of 1 s). Why are these features so important? Because, as it is well recognized in the reaction infiltration process, the nonlinear interaction between liquid (Si) flow and chemical reaction

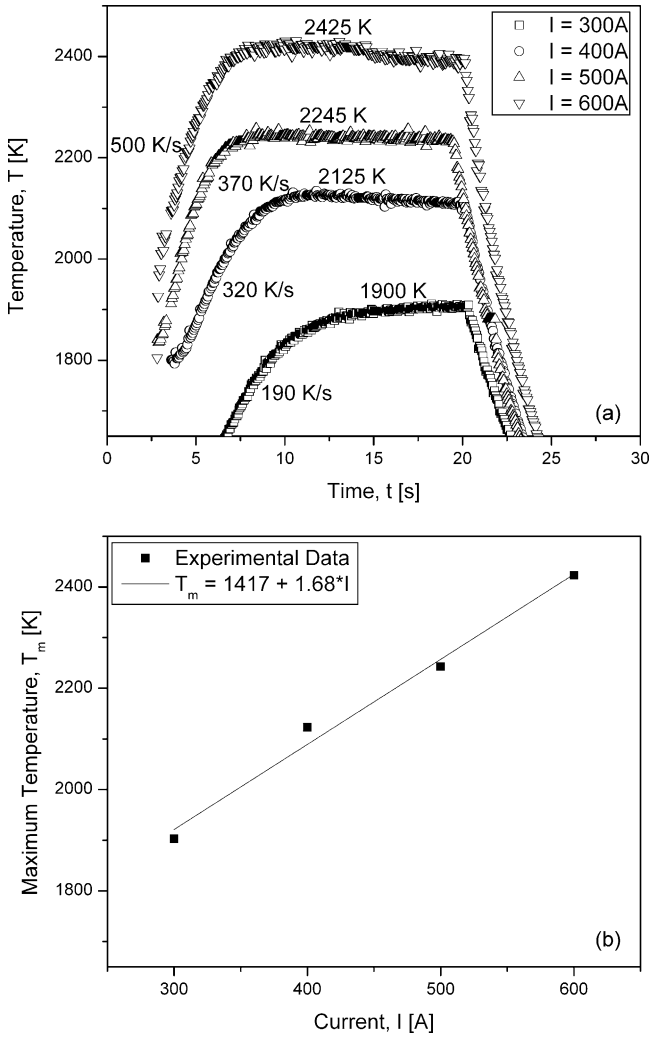

Fig. 2. (a) Typical temperature–time profiles for sample heat treatment and (b) Saturation temperature (T_m) as a function of applied current (I).

(Si + C) determines the characteristics of the resulting composite [13]. Indeed, the reaction between the infiltrating liquid silicon and carbon skeleton results in a reduction of pore size. This affects the permeability of the skeleton, reducing the infiltration velocity and may even lead to choking—cessation of silicon flow before reaching complete infiltration. Another concern, which is of critical importance for the composite properties, is causing damage to the preform skeleton. The aforementioned features which are specific to the EILI process, i.e. uniform, rapid preheating of the preform to high temperature and short process duration, provide favorable conditions for complete liquid silicon infiltration into the C/C pore structure, as well as preservation of the skeleton from damage.

3.2. Silicon infiltration

As noted above, the open porosity of the initial preform is $\phi_o = 15\%$. Assuming that silicon infiltrates into the C/C skeleton without a significant degree of conversion to SiC (see Section 3.3 for justification of this assumption for the considered conditions), it is reasonable to define the instantaneous open porosity of the skeleton (ϕ) as follows:

$$\phi = \phi_o - \left(\frac{\rho_C}{\rho_{Si}}\right)\left\{\frac{(m_2 - m_1)}{m_1}\right\}(1 - \phi_o) \quad (1)$$

where $m_{1,2}$ = mass of the sample before (1) and after (2) infiltration, and ρ_C and ρ_{Si} are theoretical densities of carbon and silicon, respectively. When $\phi = 0$, complete infiltration has been reached and thus this parameter defines the degree of infiltration. The dependence of ϕ as a function of applied electrical current, I, for 20 s of heat treatment is shown in Fig. 3a. It can be seen that ϕ decreases as the magnitude of applied current increases and then reaches saturation at I ~500 A. It is important to note that the saturation value for ϕ is close to zero which means that under these conditions essentially all open pores are filled with silicon. For a better understanding, one has to analyze the data, taking into account the temperature–time profiles shown in Fig. 2a. Two aspects

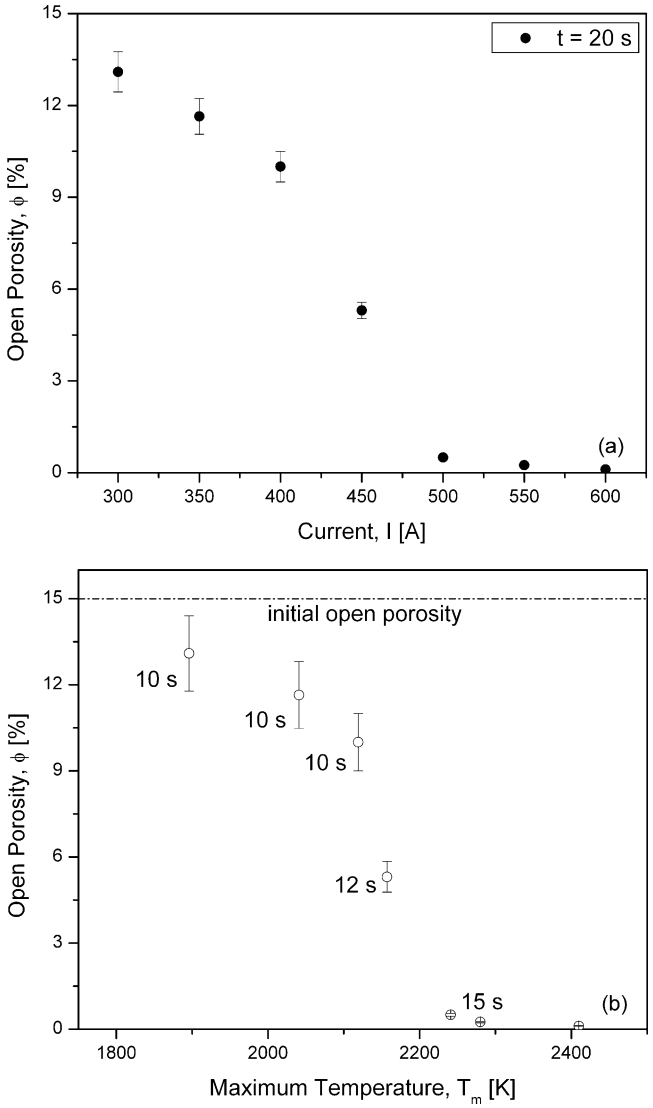

Fig. 3. Dependence of preform open porosity (ϕ) as a function of: (a) applied electrical current and (b) saturation temperature (T_m).

should be accounted for: heating rate and saturation temperature. Fig. 3b represents the same values of ϕ, but as a function of the T_m that was achieved for each specific applied electrical current. Additionally, the amount of time that the system sustained a temperature above the melting point of silicon is noted for each point.

It can be seen that lower current leads not only to a lower T_m, but also, because of a slower heating rate, a shorter duration of treatment at temperatures above 1687 K, the melting point of Si. Though in general a higher T_m (all of which are above the melting point of silicon) results in a lower ϕ, complete infiltration ($\phi = 0$) occurs after 15 s of treatment at any $T_m > 2200$ K.

In order to gain scientific insight on the infiltration process, let us consider a simple model that describes liquid silicon spreading along a carbon capillary with inner radius r_{ef}. Assuming complete wetting between silicon and carbon (which is a good assumption for two components with mutual affinity), the infiltration rate can be calculated as follows [14]:

$$\frac{dl}{dt} = \frac{\sigma}{4\mu}\frac{r_{ef}}{l} \tag{2}$$

where σ = the coefficient of surface tension for the liquid component, μ = the dynamic viscosity of the liquid, l = infiltration length, and t = time. From Eq. (2) it is easy to derive, for example, the infiltration length as a function of time:

$$l = \sqrt{\frac{\sigma}{2\mu} r_{ef} t} \tag{3}$$

The temperature dependence of σ and μ for silicon is shown in Fig. 4a [15]. While both parameters decrease with increasing temperature, their characteristic ratio from Eq. (3) actually increases slightly. This explains why the infiltration length increases with temperature. However, as one can see in Fig. 4a, this ratio does not change much, ranging from about 23 to 24, over the range of investigated temperatures (1700–2400 K), which allows us to estimate the depth of infiltration as a function of time. Assuming that r_{ef} is on the order of 10 μm (the characteristic size of the C/C pore structure), the infiltration depth is calculated according to Eq. (3) (see Fig. 4b).

The simple model used here cannot precisely describe the observed phenomenon; however, it shows that under the investigated conditions, capillary spreading of silicon is a very rapid process. In fact, it requires less than 1 s to infiltrate to a depth of 1 cm. This conclusion was confirmed by examining the cross-section of a synthesized sample, which will be discussed later. A similarly high rate was observed for so-called chemical capillary spreading. That is, spreading which occurs with the simultaneous formation of a thin layer of carbide, during the propagation of a combustion reaction in metal–carbon systems, where heating rates were comparable with those used in this work [16].

The experimental data on open porosity as a function of treatment time at a temperature above the silicon melting point (m.p.) is presented in Fig. 5. It can be seen that it requires ~8 s for complete infiltration.

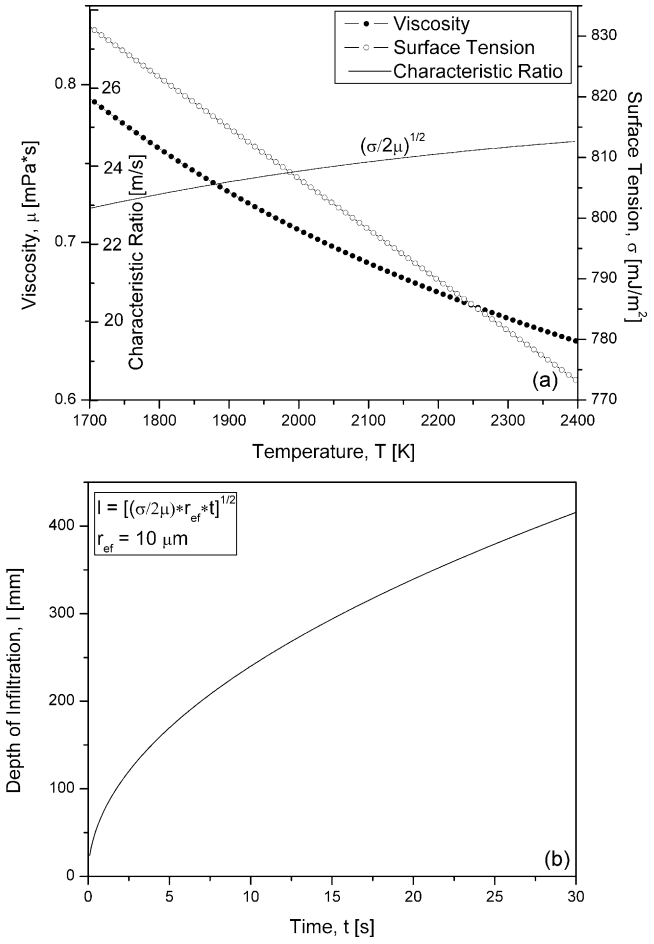

Fig. 4. (a) Temperature dependence of characteristic properties of silicon and (b) estimated infiltration length for the Si–C system.

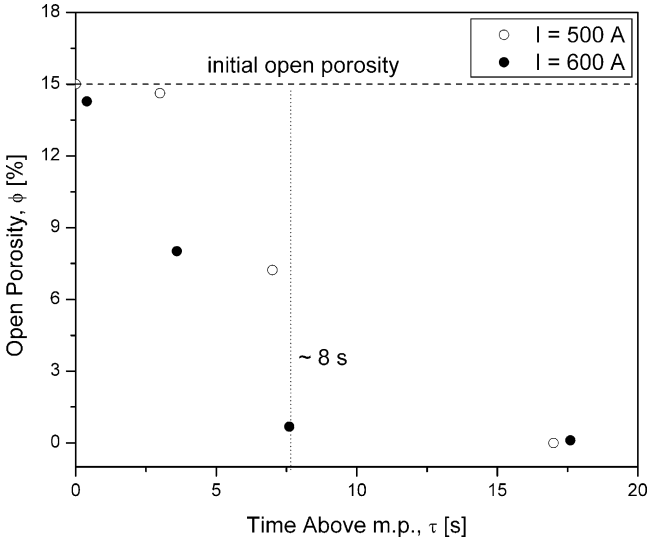

Fig. 5. Effect of silicon infiltration on the C/C composite open porosity.

Taking into account that the sample diameter is on the order of 1 cm, it can be concluded that the complex microstructure of pores in the C/C composite significantly retards the infiltration rate, compared to what might be expected from the simple model used above for rate estimations.

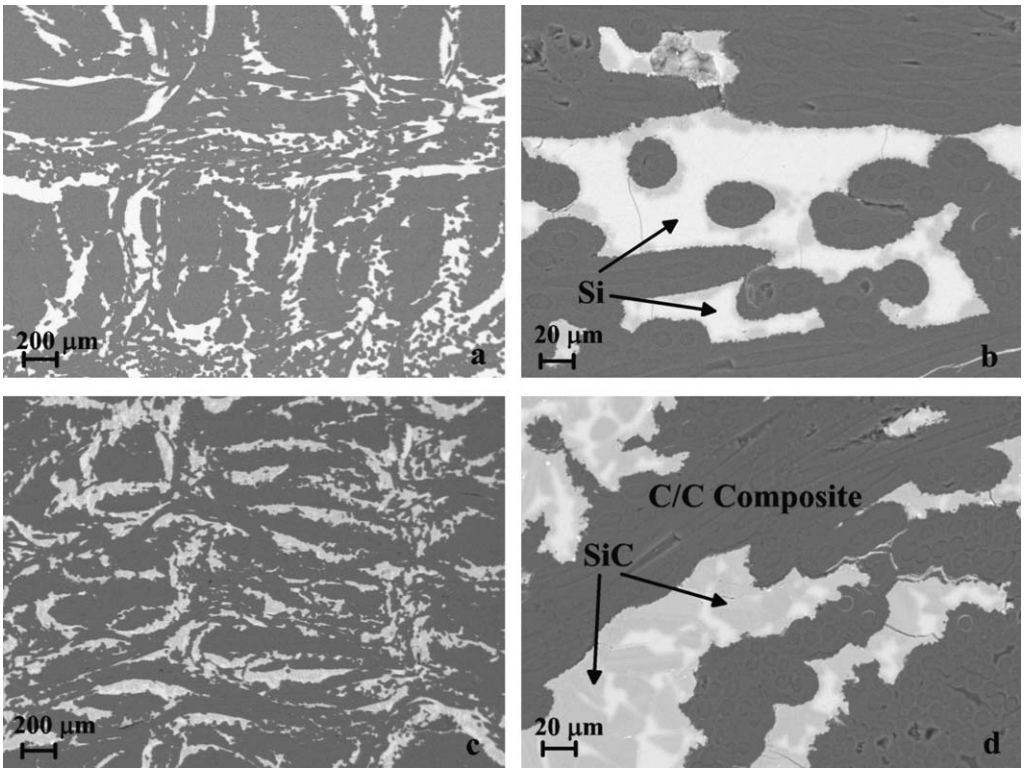

Fig. 6. Typical microstructure of composite under different heat treatment conditions: (a) and (b) 2125 K for 20 s; (c) and (d) 2425 K for 10 s.

3.3. Chemical reaction

As noted earlier, another critical process during synthesis of the composite material is the chemical interaction between liquid silicon and carbon. Fig. 6 presents a typical microstructure (backscattering mode) of the synthesized composite after heat treatment at two different temperatures, 2125 and 2425 K. It can be seen that, as concluded above, after 10 s of treatment, all pores are filled with a silicon-based phase (Fig. 6a and c). Closer inspection of the microstructures (Fig. 6b and d) shows that in contrast to the infiltration rate, the temperature has a very significant influence on the rate of chemical reaction, which is characterized by the amount of the gray phase in the figures. Note that XRD patterns of the samples showed two sets of peaks, i.e. one for Si and the other for SiC. In turn, EDS analysis of the light and gray phases in Fig. 6 reveals that the former is pure silicon, while the latter is silicon carbide. It can be seen that significantly more SiC (gray phase) was formed after 10 s at $T = 2425$ K (Fig. 6d) than after 20 s at $T = 2125$ K (Fig. 6b).

Statistical treatment of microstructures like those in Fig. 6 allows one to create a size distribution of the carbide phase for samples produced at different heat treatment temperatures (see Fig. 7). Using data shown in Fig. 7, one can estimate the kinetics of the reaction between silicon and carbon.

An overview of different kinetics models for the molten silicon–carbon system is presented in [13]. It is stated that while significant controversy regarding the exact mechanism still exists in literature, the two most feasible basic mechanisms are typically considered, i.e. diffusion through the SiC layer [7,8] and dissolution of carbon into molten silicon followed by crystallization of SiC grains [17]. Analysis of typical microstructures of the formed SiC phase indicates that while the main carbide morphology is represented by large crystals (Fig. 8a), a thin (~1 μm) SiC layer exists along the boundary of the C/C skeleton (Fig. 8b). This observation suggests that the thin carbide layer initially formed during the silicon infiltration process, while further reaction occurs due to carbon diffusion through this layer, followed by crystallization of the SiC phase.

One may estimate the kinetics parameters of the reaction using the data shown in Fig. 7. First, let us assume, as it was suggested in [18], that the reaction is limited by carbon diffusion through the solid layer and follows a parabolic law of the form:

$$x \sim \sqrt{Dt} \tag{4}$$

where x = the diffusion length, D = the diffusion coefficient, and t = time.

Also, it is recognized that diffusion coefficients through a solid layer typically follow an Arrhenius type temperature dependence:

$$D = D_0 \exp\left(-\frac{E}{RT}\right) \tag{5}$$

where D_0 = the reference diffusion coefficient, E = activation energy, R = the universal gas constant, and T = temperature. In

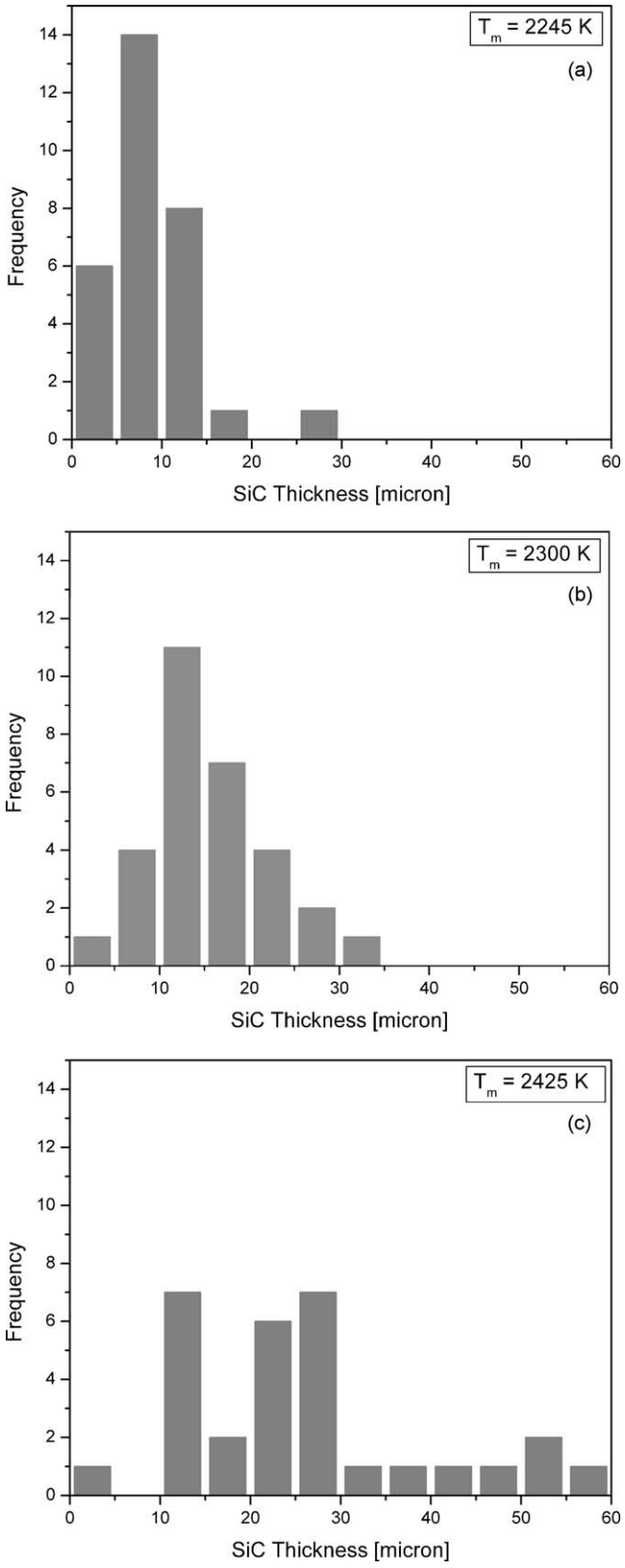

Fig. 7. Size distribution of SiC phase for 20 s of heat treatment at different temperatures: (a) 2245 K; (b) 2300 K; (c) 2425 K.

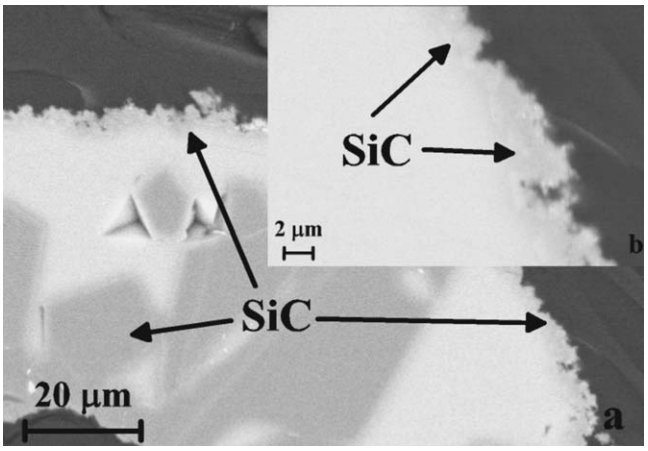

Fig. 8. Typical microstructure of the SiC phase.

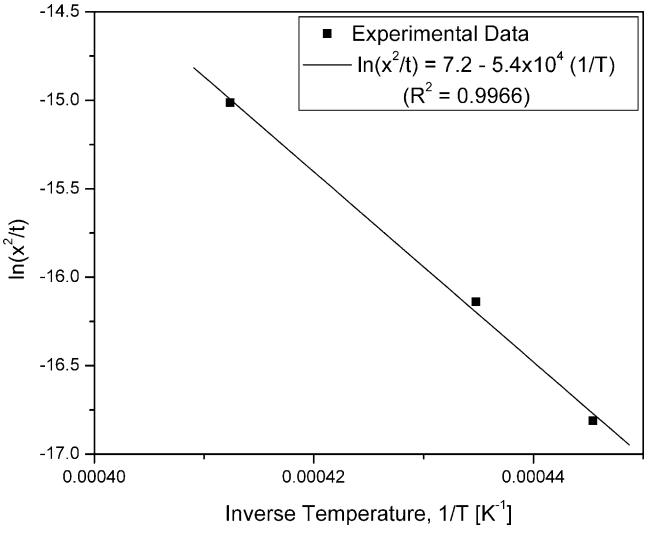

Fig. 9. Arrhenius plot resolving the kinetics of SiC formation during EILI.

this case, Eqs. (4) and (5) can be combined, revealing:

$$\ln\left(\frac{x^2}{t}\right) \sim \ln(D) = \ln(D_0) - \left(\frac{E}{R}\right)\left(\frac{1}{T}\right) \quad (6)$$

Thus, one may plot $\ln(x^2/t)$ vs. $1/T$, where x is the average size of the SiC phase taken from Fig. 7. As it is shown in Fig. 9, this dependence represents a perfectly straight line ($R^2 = 0.9966$) whose slope (under the above assumptions) contains the activation energy for carbon diffusion through the SiC layer. Using this slope, and Eq. (6), an activation energy of $E \sim 107$ kcal/mol was found, which is greater than previously reported, $E \sim 76$ kcal/mol [18]. Also, the absolute value of the diffusion coefficient at different temperatures in this work appeared to be slightly lower than those of a previous study (see Table 1). Note that all of these coefficients are in the typical range for solid state diffusion and much less than those for diffusion in melts ($\sim 10^{-5}$ cm^2/s).

The above observations of the SiC phase microstructure and evaluation of the diffusion coefficient allow us to suggest another mechanism of interaction between silicon and carbon

Table 1
Diffusion coefficients for molten silicon–carbon reaction.

Diffusion coefficient (cm^2/s)	Temperature		
	2073 K	2273 K	2373 K
D [18]	3.6×10^{-8}	9×10^{-8}	3.6×10^{-7}
D [this work]	6.5×10^{-9}	6.4×10^{-8}	1.8×10^{-7}

during the EILI process. This mechanism assumes that during infiltration of molten silicon a layer of initial SiC product forms on the surface of the solid (carbon) reactant. Further reaction proceeds by diffusion of carbon through this layer, whose thickness is assumed to remain constant during the reaction. The final product crystallizes in the volume of the melt after saturation. This type of mechanism was observed during high temperature combustion reactions [19,20] that involve similar temperature and time scales with those for EILI.

Thus, one may conclude that during EILI, silicon rapidly infiltrates through the open pore skeleton of the preform, reaching complete infiltration before reaction between Si and carbon can significantly affect the infiltration process. Infiltration is followed by the formation of a SiC phase at relatively slow rates which are close to that observed for solid state diffusion. Microstructural studies suggest that the controlling mechanism is diffusion of carbon through an initial SiC layer to the molten silicon. One should also note that because the total duration of the entire process is on the order of 20 s no damage to the carbon skeleton was observed.

3.4. Mechanical properties

It is important from an application standpoint to consider how EILI processing influences the mechanical properties of the composite material. In order to quantify this, several specimens of the initial C/C composite and samples produced with varying heat treatment conditions were tested under a compressive load. As noted previously, the initial preform has only about 15% open porosity. Thus, even under conditions of complete infiltration and silicon conversion to the SiC phase, one cannot form a continuous carbide skeleton. The compressive strength of the materials as a function of applied electrical current ($t = 20$ s) used for heat treatment is shown in Fig. 10. It can be seen that composites synthesized under optimal conditions ($I > 500$ A) possess twice the compressive strength compared to the initial C/C material. One more parameter that can significantly improve the properties of the final material is the application of an external load during synthesis. The considered apparatus has a unique ability to precisely time (within ~0.1 s increments) and rapidly apply (response time ~10 ms) a uniaxial load (250–35,000 N) to the sample. An investigation into the optimization of the load-time schedule for EILI synthesis of C/C–SiC composite is currently underway.

3.5. Process characterization

The considered EILI method for material synthesis involves several processes, including electrical preheating of the reactants (C/C composite and silicon powder), infiltration of molten silicon into the porous carbon structure, and silicon–carbon chemical interaction. The results reported here show that under the investigated conditions, the characteristic time and length scales for these processes are:

(i) Preheating, $t_h \sim 3$–5 s, $l_h \sim 1$ cm.
(ii) Silicon infiltration into the C/C composite pore structure, $t_{inf} \sim 1$–5 s, $l_{inf} \sim 1$ cm.
(iii) Reaction, $t_r \sim 10$–20 s, $l_r \sim 10$–20 μm.

Thus, it can be concluded that the limiting stage of the synthesis process is the reaction to produce a SiC phase. This feature favors completely filling the pore structure with silicon before a significant amount of solid SiC phase is formed. The latter process can prevent Si infiltration (choking) by reducing the pore size and closing off the open pore structure. The duration of heat treatment above the melting point of silicon necessary for full conversion to SiC is on the order of 15–20 s and thus the microstructure of the initial C/C skeleton remains undamaged. Discussion on how the magnitude of the applied current (i.e. varying the heat treatment conditions) influences the rate of infiltration and chemical reaction was covered earlier. It was found that higher current leads to a more rapid preheating rate, and higher saturation temperature, resulting in faster infiltration and chemical reaction rates.

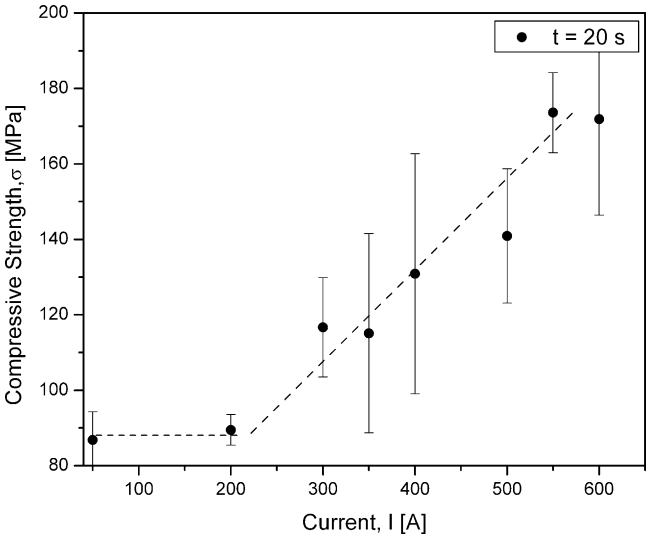

Fig. 10. Dependence of composite compressive strength on applied electrical current.

3.6. Surface coating

The EILI approach can also be used for the synthesis of a protective layer on the outer surface of the carbon/carbon composite. Indeed, for many high-temperature applications, including brakes, it is important to protect carbon articles from oxidation. Typically, for this purpose a coating, which may range from one to several layers, containing silicon carbide is formed on the surface of the considered material. This process involves spreading a silicon-based slurry on the sample surface

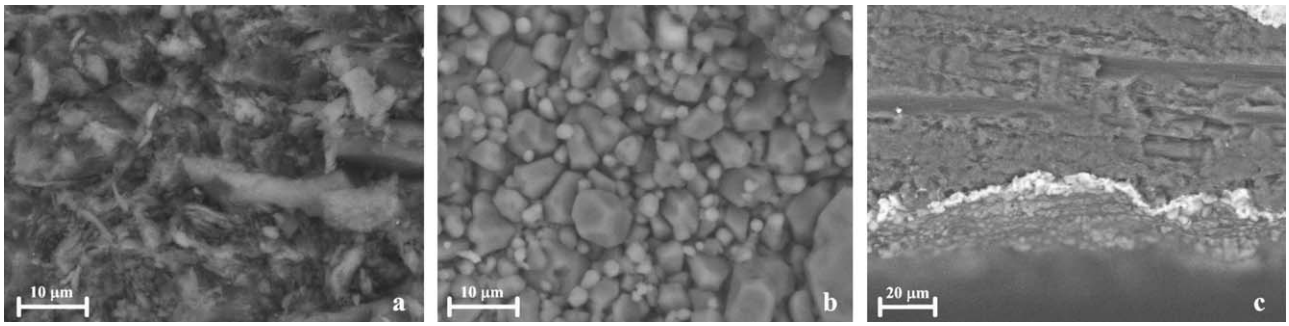

Fig. 11. Microstructures of the surface of the composite (a) before and (b and c) after formation of a thin protective SiC layer.

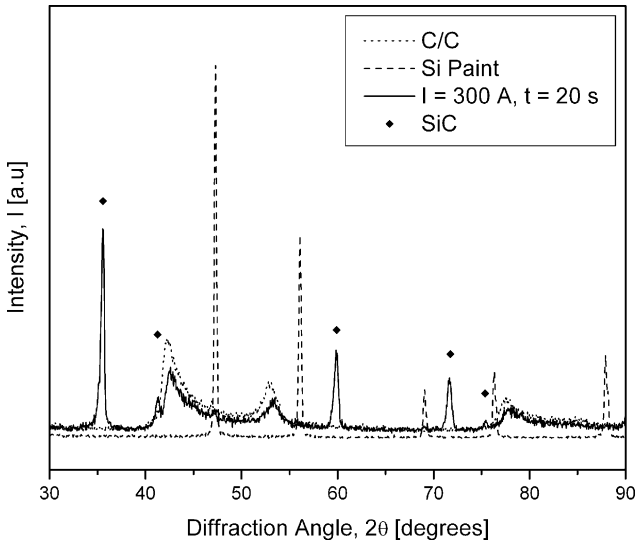

Fig. 12. XRD patterns of the surface of initial C/C composite, silicon slurry, and composite surface after SiC formation.

followed by a relatively long term, high-temperature treatment in a furnace under an inert atmosphere [21].

Our experiments show that by optimizing the conditions of the EILI process, one may produce a thin SiC layer on the surface of the C/C composite in the time range 10–20 s. Fig. 11 demonstrates the microstructure of the initial C/C composite surface (a), as well as after formation of a SiC layer (b) using the procedure described in Section 2. It can be seen that using a relatively small amount of silicon pasted on the sample surface together with a relatively low electrical current (300–350 A), one may produce a thin (∼5 μm; see Fig. 11c) layer that consists of fine (∼5 μm) grains (Fig. 11b) of silicon carbide. The latter was confirmed through XRD analysis, which is shown in Fig. 12. For a sample treated for 20 s with a current of I = 300 A, XRD indicates only SiC and C peaks. It is clear that carbon peaks were detected because the thickness of the produced SiC layer (5–10 μm) is smaller than the depth of X-ray penetration (∼50 μm).

4. Concluding remarks

EILI is a novel method for the production of C/C–SiC composite. Though the complex pore structure of the C/C composite used here affects the rate of silicon infiltration, it was found that the fast preheating of the EILI approach allows rapid (∼seconds) infiltration of a less refractory material (Si) into a porous solid (C) structure, followed by conversion of the silicon into silicon carbide without damaging the microstructure of the preform. Mechanical testing of EILI-synthesized materials showed that they posses much greater (∼2X) mechanical properties as compared to the initial C/C composite. It was also demonstrated that EILI is an effective approach for the formation of a thin refractory layer on the material surface. It is important to note that this method could be applied to other carbide forming elements, such as titanium, zirconium, tungsten, etc. All of the aforementioned features make EILI a powerful tool for the synthesis of a variety of carbon-based materials.

References

[1] F. Christin, Design, fabrication, and application of thermostructural composites (TSC) like C/C, C/SiC, and SiC/SiC composites, Adv. Eng. Mater. 4 (12) (2002) 903–912.
[2] J.F. Huang, F. Deng, X.B. Xiong, H.J. Li, K.Z. Li, L.Y. Cao, J.P. Wu, High performance Si–SiC composite coating for C/C composites prepared by a two-step pack cementation process, Adv. Eng. Mater. 9 (4) (2007) 322–324.
[3] W. Krenkel, F. Berndt, C/C–SiC composites for space applications and advanced friction systems, Mater. Sci. Eng. A 412 (1–2) (2005) 177–181.
[4] K. Krnel, Z. Stadler, T. Kosmac, Preparation and properties of C/C–SiC nano-composites, J. Eur. Ceram. Soc. 27 (2–3) (2007) 1211–1216.
[5] C. Evans, A. Parmee, R. Rainbow, Silicon treatment of carbon fibre–carbon composites, in: Proceedings of 4th London Conference on Carbon and Graphite, 1974, pp. 231–235.
[6] W. Hillig, R. Mehan, C. Morelock, V. DeCarlo, W. Laskow, Silicon/silicon carbide composites, Am. Ceram. Soc. Bull. 54 (12) (1975) 1054–1056.
[7] E. Fitzer, A. Gkogkidis, Fiber-reinforced silicon-carbide, Am. Ceram. Soc. Bull. 65 (2) (1986) 326–335.
[8] M.E. Washburn, W.S. Coblenz, Reaction-formed ceramics, Am. Ceram. Soc. Bull. 67 (2) (1988) 356–363.
[9] Y.M. Chiang, R.P. Messner, C.D. Terwilliger, D.R. Behrendt, Reaction-formed silicon-carbide, Mater. Sci. Eng. A 144 (1991) 63–74.
[10] M. Singh, D.R. Behrendt, Microstructure and mechanical-properties of reaction-formed silicon-carbide (RFSC) ceramics, Mater. Sci. Eng. A 187 (2) (1994) 183–187.
[11] P. Sangsuwan, S.N. Tewari, J.E. Gatica, M. Singh, R. Dickerson, Reactive infiltration of silicon melt through microporous amorphous carbon preforms, Metall. Mater. Trans. A 30 (5) (1999) 933–944.

[12] J.D.E. White, A.S. Mukasyan, M.L. La Forest, A.H. Simpson, Novel apparatus for joining of carbon–carbon composites, Rev. Sci. Instrum. 78 (1) (2007) 015105.
[13] P. Sangsuwan, J.A. Orejas, J.E. Gatica, S.N. Tewari, M. Singh, Reaction-bonded silicon carbide by reactive infiltration, Ind. Eng. Chem. Res. 40 (23) (2001) 5191–5198.
[14] V.G. Levich, Physicochemical Hydrodynamics, Prentice-Hall, Inc., Englewood Cliffs, NJ, 1962, p. 383.
[15] V. Kostikov, A. Varenkov, Super-high-temperature Composite Materials, Intermet Engineering, Moscow, 2003, p. 320.
[16] A.G. Merzhanov, A.S. Rogachev, A.S. Mukasyan, B.M. Khusib, Macrokinetics of structural transformation during the gasless combustion of a titanium and carbon powder mixture, Combust. Explo. Shock+ 26 (1) (1990) 92–102.
[17] R. Pampuch, E. Walasek, J. Bialoskorski, Reaction-mechanism in carbon liquid silicon systems at elevated-temperatures, Ceram. Int. 12 (2) (1986) 99–106.
[18] V. Kostikov, A. Varenkov, Super-high-temperature Composite Materials, Intermet Engineering, Moscow, 2003, p. 324.
[19] V.V. Alexandrov, M.A. Korchagin, Mechanism and macrokinetics of reaction accompanying the combustion of SHS systems, Combust. Explo. Shock+ 23 (5) (1988) 557–564.
[20] A.M. Kanury, A kinetics model for metal + nonmetal reactions, Metall. Trans. A 23 (1992) 2349–2356.
[21] F. Smeacetto, M. Salvo, M. Ferraris, Oxidation protective multilayer coatings for carbon–carbon composites, Carbon 40 (4) (2002) 583–587.